PAULING, L. (1960). *The Nature of the Chemical Bond*, p. 228. Ithaca: Cornell Univ. Press.

POPLE, J. A. & BEVERIDGE, D. L. (1970). *Approximate Molecular Orbital Theory*. New York: McGraw-Hill. Using Quantum Chemistry Program Exchange, Program No. 141, Univ. of Indiana, Bloomington.

PRUSINER, P., BRENNAN, T. & SUNDARALINGAM, M. (1973). *Biochemistry*, **12**, 1196–1202.

PRUSOFF, W. H., LAJTH, L. G. & WELCH, A. D. (1956). *Biochim. Biophys. Acta*, **20**, 209–214.

PULLMAN, B. & BERTHOD, H. (1972). *FEBS Lett.* **20**, 341–343.

PURNELL, L. G., ESTES, E. D. & HODGSON, D. J. (1976). *J. Am. Chem. Soc.* **98**, 740–743.

ROBINS, M. J., CURRIE, B. L., ROBINS, R. K. & BLOCH, A. (1969). *Proc. Am. Assoc. Cancer Res.* **10**, 73.

ROBLIN, R. O., LAMPEN, J. O., ENGLISH, J. P., COLE, Q. P. & VAUGHAN, J. R. (1945). *J. Am. Chem. Soc.* **67**, 290–294.

SCHANNON, W. M., ARNETT, G. & SCHABEL, F. M. (1972). *Antimicrob. Agents Chemother.* **2**, 159–163.

SCHWALBE, C. H. & SAENGER, W. (1973*a*). *Acta Cryst.* B**29**, 61–69.

SCHWALBE, C. H. & SAENGER, W. (1973*b*). *J. Mol. Biol.* **75**, 129–143.

SINGH, P. & HODGSON, D. J. (1974*a*). *Acta Cryst.* B**30**, 1430–1435.

SINGH, P. & HODGSON, D. J. (1974*b*). *Biochemistry*, **13**, 5445–5452.

SINGH, P. & HODGSON, D. J. (1975). *Acta Cryst.* B**31**, 2519–2521.

SINGH, P. & HODGSON, D. J. (1977). *J. Am. Chem. Soc.* **99**, 4807–4815.

SKODA, J. (1963). *Prog. Nucleic Acid Res. Mol. Biol.* **2**, 197–219.

SPRANG, S., SCHELLER, R., ROHRER, D. & SUNDARALINGAM, M. (1978). *J. Am. Chem. Soc.* **100**, 2867–2872.

STEWART, R. F. & JENSEN, L. H. (1964). *J. Chem. Phys.* **40**, 2071–2075.

STEWART, R. F. & JENSEN, L. H. (1967). *Acta Cryst.* **23**, 1102–1105.

SUNDARALINGAM, M. (1965). *J. Am. Chem. Soc.* **87**, 599–606.

SUNDARALINGAM, M. (1969). *Biopolymers*, **7**, 821–860.

SUNDARALINGAM, M. (1972). *Jerusalem Symp. Quantum Chem. Biochem.* **4**, 73–98.

SUNDARALINGAM, M. (1973). *Jerusalem Symp. Quantum Chem. Biochem.* **5**, 417–455.

WANG, M. C. & BLOCH, A. (1972). *Biochem. Pharmacol.* **21**, 1063–1073.

YOUNG, D. W., TOLLIN, P. & WILSON, H. R. (1969). *Acta Cryst.* B**25**, 1423–1432.

ZACHARIASEN, W. H. (1963). *Acta Cryst.* **16**, 1139–1144.

ZACHARIASEN, W. H. (1968). *Acta Cryst.* A**24**, 212–216.

Acta Cryst. (1981). B**37**, 1584–1591

The Charge Density and Hydrogen Bonding in 9-Methyladenine at 126 K

BY B. M. CRAVEN

Department of Crystallography, University of Pittsburgh, Pittsburgh, Pennsylvania 15260, *USA*

AND P. BENCI

Department of Chemistry, Carnegie–Mellon University, Pittsburgh, Pennsylvania 15213, *USA*

(*Received* 12 *May* 1980; *accepted* 10 *February* 1981)

Abstract

The charge density distribution in the crystal structure of 9-methyladenine at 126 K has been determined from X-ray diffraction data (Mo $K\alpha$) for 4002 reflections with $F > 3\sigma(F)$ and $\sin\theta/\lambda < 1{\cdot}0$ Å^{-1}. The nuclear positional parameters for all atoms, and anisotropic thermal parameters for the H atoms were assumed to have values determined from a previous neutron structure determination. The electronic charge density was analyzed in terms of Stewart's rigid pseudoatom model, using restricted Slater radial functions and complete angular multipole terms extending to octapoles for C and N and quadrupoles for H pseudoatoms. The least-squares refinement converged with $R_w = 0{\cdot}030$. The net charges on atoms N(1), N(7) and N(3) are consistent with this order of decreasing preference as sites for hydrogen bonding and protonation of adenine derivatives. In the purine C—N bonds there is a correlation between decreasing peak deformation density and increasing bond length. The charge distribution in the two NH···N interactions is consistent with the importance of Coulombic interactions for hydrogen bonding. There are dipole deformations at the C—H and N—H hydrogen atoms which enhance the charge density in the bonding region. Unexpectedly,

0567-7408/81/081584-08$01.00

these deformations are significantly stronger for the C–H groups. It is suggested that these polarizations are involved in the short C(8)–H(8)···O interactions which occur in the crystal structures of several purine derivatives.

Introduction

An electronic charge density study of 9-methyladenine has been carried out to obtain a better understanding of the electronic structure and hydrogen-bonding behavior of the adenine moiety in nucleic acids and nucleotides. Earlier X-ray crystal structure determinations of 9-methyladenine involved room-temperature data (Stewart & Jensen, 1964; Kistenmacher & Rossi, 1977). We considered it necessary to collect diffraction data at low temperature so as to minimize systematic errors in deconvoluting the charge distribution from the atomic thermal vibrations.

McMullan, Benci & Craven (1980) (hereafter MBC) have determined the neutron structure of 9-methyladenine at 126 K to obtain values for the nuclear positional and anisotropic thermal parameters. These results are of critical importance for the present interpretation of the electronic charge density around the protons.

Experimental

Crystals of 9-methyladenine were grown by slow cooling (370 K to 298 K) of an aqueous solution contained in a Dewar flask. All X-ray data were measured using a crystal elongated on the a axis showing the forms {100} and {011}. The crystal was symmetrically developed according to the crystal class $2/m$ so that the distances of faces from a common origin were 0·26 and 0·13 mm for the forms {100} and {011} respectively.

The crystal was mounted with a along the φ axis of an Enraf–Nonius CAD-4 computer-controlled diffractometer. The X-radiation was Mo $K\alpha$ (λ = 0·7093 Å) obtained by 002 reflection from a graphite monochromator. The crystal was cooled in a stream of nitrogen gas provided by an Enraf–Nonius low-temperature device. To minimize ice formation on the crystal, the diffractometer was in a sealed glass box together with four containers of phosphorus pentoxide. The temperature was monitored ($\pm$2 K) using a thermocouple in the cold stream 8 mm from the crystal.

The aim was to collect X-ray data with the crystal as nearly as possible at the temperature (126 $\pm$ 1 K) used by MBC for the neutron data collection. Initially, the apparent temperature was checked by comparing the X-ray and neutron values for the unit-cell parameters, particularly a. The neutron measurements had shown this to be the only cell parameter that was significantly temperature-sensitive, with $\Delta a = -0{\cdot}015$ (1) Å in the range of interest, 136 to 116 K.* The MBC neutron values at 126 K were a = 7·505 (1), b = 12·285 (2), c = 8·482 (1) Å, β = 122·82 (1)°. The following cell parameters were presently obtained by least-squares fit of $\sin^2\theta$ values for 25 X-ray reflections in the range $17 < \theta < 33°$ which were measured at $\pm\omega$. At 130 K, a = 7·510 (4), b = 12·283 (7), c = 8·489 (4) Å, β = 122·78 (3)°, and at 124 K, a = 7·504 (3), b = 12·287 (7), c = 8·484 (4) Å, β = 122·83 (3)°. The X-ray intensity data were collected with the temperature reading 126 K, since it was believed that this would match the temperature of the neutron data collection within about $\pm$5 K. The more accurate neutron cell parameters for 126 K were used in the X-ray structure refinement.

Integrated X-ray intensities were measured by $\omega/2\theta$ scans with a scan width $\Delta(2\theta) = (2{\cdot}4 + 0{\cdot}7 \tan\theta)°$. Throughout the 21 days of data collection, the intensities of three standard reflections were monitored after every 75 reflections. Variations in these intensities were insignificant. There were a total of 6583 reflections measured within $(\sin\theta/\lambda)_{max} = 1{\cdot}0$ Å^{-1}, of which 5277 were not duplicate or symmetry-related. The intensities were corrected for X-ray absorption ($\mu = 0{\cdot}099$ mm^{-1}) using a numerical integration procedure (Busing & Levy, 1957) which also provided values of the mean crystal path lengths $\bar{t}$ for use in calculating extinction factors. Absorption factors were in the range 0·96 to 0·98 and $\bar{t}$ in the range 0·19 to 0·35 mm. The variance of an integrated intensity (I) was taken to be $\sigma^2(I) = \sigma^2 + (0{\cdot}02I)^2$, where σ^2 was the variance due to counting statistics. There were 4002 reflections with $F > 3\sigma(F)$, and only these were used in the structure refinement.

In the later stages of the structure refinement, it was suspected that the variances might have been underestimated for reflections in the weaker to medium range of intensity and overestimated for very weak reflections. This was supported by a study of the 256 reflections for which duplicate intensity measurements had been made. The variances were redefined as $\sigma^2(F) = (818 - 48F + 10{\cdot}5F^2) \times 10^{-4}$, where the constants were obtained from a least-squares fit involving these reflections. The residual which was minimized was $\sum_{j=1}^{256}[\sigma^2(F_j) - \Delta_j^2/2]^2$ where $F_j = (F_1 + F_2)/2$ and $\Delta_j = |F_1 - F_2|$ and F_1 and F_2 were observed structure amplitudes for the jth reflection.

Results

The electronic charge density refinement was based on the rigid pseudoatom model of Stewart (1976). C and N

* The molecules lie in sheets parallel to (100). The temperature sensitivity in a is attributed to the relative weakness of intermolecular forces between sheets.

pseudoatoms were assumed to have spherical 'K-shell X-ray scattering factors based on self-consistent-field wavefunctions (Clementi, 1965). Valence-shell scattering factors included radial charge density functions of the Slater type, $[4\pi(n+2)!]^{-1}\alpha^{n+3}r^n\exp(-\alpha r)$ where $n = 0$, 1, 2 or 3 and α is a radial parameter which is a least-squares variable having different values for C, N or H. The explicit radial functions used in the pseudoatom scattering factors as well as the angular multipole terms were the same as those given in detail for the case of parabanic acid (Craven & McMullan, 1979).

For each C and N pseudoatom, there were 16 electronic population parameters which were least-squares variables. These may be regarded as the weights assigned to one monopole (p_v) and three dipole (d_j), five quadrupole (q_j) and seven octapole (o_j) deformations of the valence charge density. For each H pseudoatom, there were only nine population parameters, because octapole deformations were neglected.

Also included in the structure model were a scale factor, an isotropic extinction parameter and the nuclear positional and anisotropic thermal parameters. The extinction model was that of Becker & Coppens (1974), assuming the crystal to be of type I with a Lorentzian distribution of mosaicity. The least-squares refinement minimized the function $\sum w\Delta^2$ where $\Delta = |F_o| - |F_c|$ and $w = 1/\sigma^2(F_o)$. This was carried out with the computer program of Craven & Weber (1977) which permits the variables to be grouped in blocks of different size and constituency, including a full-matrix refinement as the limiting case. For 9-methyladenine, refinement was expedited by using two large parameter blocks. The first consisted of the scale factor, the extinction parameter, the three radial parameters, all monopole and quadrupole population parameters and the anisotropic thermal parameters for C and N atoms, giving a total of 179 variables. The second consisted of the dipole and octapole population parameters giving a total of 131 variables.* Throughout the refinement, all positional parameters and the H atom anisotropic thermal parameters were fixed at the neutron values of MBC. A first refinement gave convergence at $R = 0.036$, $R_w = 0.031$, QME = 1·387.†

A residual electron density map was calculated as a difference Fourier synthesis with $(F_o - F_c)$ coefficients. Several features in this map appeared to be very significant in terms of the e.s.d. in the residual density, which had the average value 0·04 e Å^{-3} over the unit cell. This map is not shown here, but it was similar to a subsequent map (Fig. 1). The most significant feature (7σ) was the density trough (−0·30 e Å^{-3}) found near the C(2)—N(3) bond, above the molecular plane (Fig. 1*a*). The contribution to this trough was −0·08 e Å^{-3} or $4{\cdot}2\sigma$ from the 1353 non-symmetry-related reflections with $\sin\theta/\lambda < 0{\cdot}6$ Å^{-1} and −0·22 e Å^{-3} or $5{\cdot}5\sigma$ from the remaining 2649 reflections with $\sin\theta/\lambda \geq 0{\cdot}65$ Å^{-1}. Thus, the trough could not be clearly attributed to either those reflections which are most sensitive to the valence charge density ($\sin\theta/\lambda < 0{\cdot}65$ Å^{-1}), or those most sensitive to the core charge density. The same was true of the other significant features in the residual density. Also, these features were difficult to relate to the atomic arrangement in a systematic way. It was

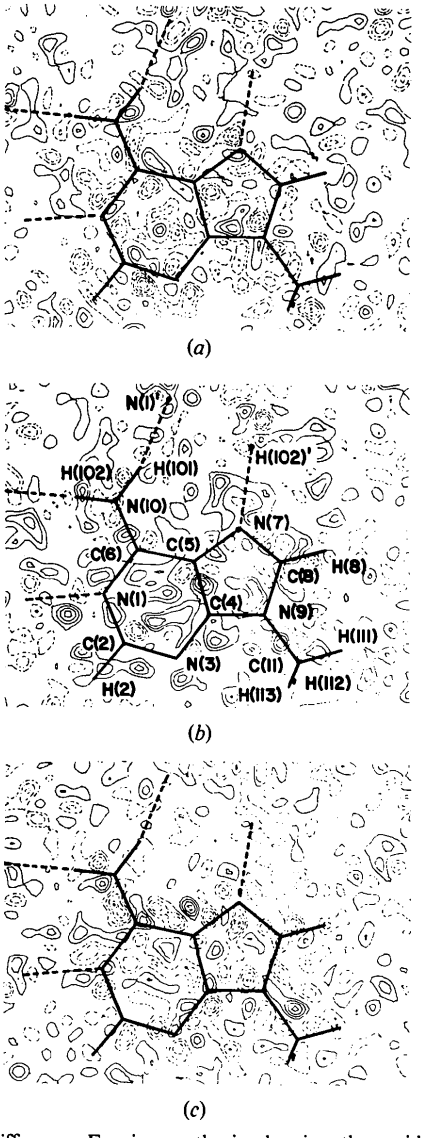

(*a*)

(*b*)

(*c*)

Fig. 1. Difference Fourier synthesis showing the residual charge density in planes (*a*) 0·4 Å above the best least-squares plane through the atoms of one molecule, (*b*) in this plane, and (*c*) 0·4 Å below it. Contours are at intervals 0·05 e Å^{-3} with zero contour omitted. The average e.s.d. in the residual density is 0·055 e Å^{-3}.

* The largest correlation between least-squares variables was found to be 0·70 for U_{11} and U_{13} of atom N(10).

† $R = \sum|\Delta|/\sum F_o$; $R_w = (\sum w\Delta^2/\sum wF_o^2)^{1/2}$; QME = $[\sum w\Delta^2/(n_{obs} - n_{param})]^{1/2}$.

concluded that, at least in part, the apparent significance of the residual density might be due to the use of inappropriate $\sigma(F)$ values.

The refinement was repeated with values of $\sigma(F)$ revised as described in the previous section, to give convergence at $R = 0{\cdot}036$, $R_w = 0{\cdot}030$, QME = $1{\cdot}180$. Structure-parameter changes from the values of the previous refinement were at most marginally significant. The residual charge density map (Fig. 1) was also similar, although the average e.s.d. was increased to 0·05 e Å^{-3}. The average e.s.d. in the residual density throughout the unit cell was 0·03 e Å^{-3} when only those reflections which are sensitive to the valence charge density ($\sin\theta/\lambda < 0{\cdot}65$ Å^{-1}) were considered. These reflections contribute $-0{\cdot}10$ e Å^{-3} to the trough near C(2)—N(3), which is the most significant feature ($3{\cdot}6\sigma$). No other exceeds $2{\cdot}5\sigma$.

Another refinement was carried out in which the C and N atom positional parameters were additional variables. The most significant shifts (0·004 Å, $2{\cdot}8\sigma$) were obtained for the x parameters for N(1), N(7) and C(8).* For the last two refinements, the R-factor ratio was 1·018 indicating that the 33 new variables gave an improvement in the model which could be accepted with 99·5% confidence (Hamilton, 1974). However, the improved agreement was obtained for reflections with large $\sin\theta/\lambda$, so that there were no significant changes either in the charge density parameters or in the largest features of the residual charge density map. It was decided to present detailed results only for the refinement (Table 1)* based on fixed neutron values for all positional parameters.

* The X-ray values for C and N atom positional parameters, along with lists of observed and calculated structure factors, have been deposited with the British Library Lending Division as Supplementary Publication No. SUP 35971 (45 pp.). Copies may be obtained through The Executive Secretary, International Union of Crystallography, 5 Abbey Square, Chester CH1 2HU, England.

Table 1. *Anisotropic thermal parameters*

These values were obtained in a structure refinement using X-ray data, in which fixed neutron values (McMullan, Benci & Craven, 1980) were assumed for all atomic positional parameters and for H-atom anisotropic thermal parameters. The values of U_{ij} (Å$^2 \times 10^4$) are defined by the temperature factor expression: $T = \exp(-2\pi^2 \sum_i \sum_j h_i h_j a_i^* a_j^* U_{ij})$.

	U_{11}	U_{22}	U_{33}	U_{12}	U_{13}	U_{23}
N(1)	188 (3)	124 (2)	102 (2)	−4 (2)	87 (2)	−2 (2)
N(3)	187 (3)	116 (2)	127 (2)	11 (2)	88 (2)	25 (2)
N(7)	232 (3)	106 (2)	121 (2)	1 (2)	118 (2)	−1 (2)
N(9)	172 (3)	97 (2)	142 (2)	9 (2)	96 (2)	−4 (2)
N(10)	293 (4)	94 (2)	145 (2)	8 (2)	147 (3)	2 (2)
C(2)	197 (3)	141 (3)	107 (2)	1 (2)	88 (2)	18 (2)
C(4)	142 (2)	98 (2)	110 (2)	2 (2)	72 (2)	5 (2)
C(5)	158 (3)	95 (2)	102 (2)	−1 (2)	80 (2)	0 (2)
C(6)	168 (3)	101 (2)	102 (2)	−1 (2)	85 (2)	−3 (2)
C(8)	227 (2)	119 (2)	140 (2)	2 (2)	120 (2)	−13 (2)
C(11)	253 (4)	102 (2)	220 (3)	23 (2)	129 (3)	−1 (2)

Table 2. *Valence electron population and radial parameters*

The unconstrained least-squares refinement gave $\sum p_v = 54{\cdot}1$ (2) for the net valence charge. Values for the population parameters given here have been scaled by the factor 56/54·1 = 1·035 so as to correspond to an electrically neutral molecule. All except p_v values are $\times 10^2$. Least-squares values for the radial parameters in the Slater-type radial density functions were $\alpha_C = 3{\cdot}292$ (12), $\alpha_N = 3{\cdot}844$ (10) and $\alpha_H = 2{\cdot}38$ (3) bohr^{-1} (Bohr radius $\simeq 0{\cdot}529 \times 10^{-10}$ m).

	p_v	d_1	d_2	d_3	q_1	q_2	q_3	q_4	q_5	o_1	o_2	o_3	o_4	o_5	o_6	o_7
N(1)	5·28 (3)	−45 (4)	23 (4)	17 (4)	−38 (8)	−61 (16)	28 (16)	−9 (16)	−11 (4)	25 (9)	28 (9)	−86 (21)	−154 (44)	15 (7)	32 (7)	−11 (5)
N(3)	5·08 (3)	−37 (4)	−33 (4)	25 (4)	−31 (8)	−26 (16)	46 (16)	−23 (15)	−17 (4)	16 (9)	5 (9)	−33 (21)	−105 (45)	8 (7)	19 (7)	−20 (6)
N(7)	5·16 (3)	17 (4)	23 (4)	−12 (4)	−48 (8)	−4 (17)	3 (16)	−47 (15)	−2 (4)	−24 (9)	17 (9)	−5 (21)	−26 (45)	−25 (7)	18 (7)	27 (6)
N(9)	5·23 (3)	8 (4)	18 (4)	15 (4)	−2 (8)	−54 (16)	40 (16)	4 (16)	−7 (4)	−10 (9)	45 (9)	−67 (23)	−160 (44)	−10 (7)	55 (7)	−18 (6)
N(10)	5·23 (3)	7 (5)	12 (5)	−2 (5)	−8 (8)	−13 (17)	13 (17)	16 (16)	−11 (4)	30 (10)	41 (10)	−166 (24)	−331 (48)	11 (8)	38 (8)	0 (7)
C(2)	3·91 (4)	18 (5)	−5 (7)	−7 (6)	−47 (8)	−47 (18)	−69 (16)	−13 (17)	3 (4)	−8 (11)	−29 (11)	163 (25)	244 (55)	−24 (8)	−24 (9)	33 (7)
C(4)	3·90 (4)	4 (6)	29 (6)	10 (6)	−32 (8)	−3 (16)	−40 (16)	−80 (16)	14 (4)	−12 (10)	−25 (10)	117 (23)	134 (51)	−30 (8)	−49 (8)	44 (7)
C(5)	3·98 (4)	−56 (6)	−23 (6)	11 (6)	−40 (8)	−38 (16)	−6 (16)	−17 (16)	−9 (4)	45 (10)	36 (10)	−194 (23)	−198 (50)	15 (8)	−4 (8)	−53 (7)
C(6)	3·86 (4)	16 (6)	−28 (6)	2 (6)	−69 (8)	−74 (17)	−101 (16)	−28 (16)	−2 (4)	−29 (10)	−48 (10)	71 (10)	273 (53)	2 (8)	−57 (8)	37 (7)
C(8)	3·90 (4)	4 (7)	38 (7)	34 (6)	−21 (8)	−80 (17)	−30 (16)	19 (17)	1 (4)	24 (10)	−31 (11)	−136 (27)	259 (54)	3 (8)	−77 (8)	0 (7)
C(11)	3·83 (4)	−1 (8)	−28 (7)	4 (8)	19 (8)	8 (18)	42 (18)	48 (17)	2 (6)	46 (13)	−87 (12)	98 (34)	174 (64)	51 (9)	−19 (9)	10 (10)
H(2)	1·01 (4)	15 (8)	−3 (7)	−75 (7)	−2 (11)	−10 (24)	−38 (21)	−40 (23)	7 (7)							
H(8)	1·05 (3)	−23 (8)	23 (7)	73 (7)	−32 (11)	1 (23)	−124 (22)	20 (23)	−7 (7)							
H(101)	0·77 (3)	−7 (7)	−21 (7)	23 (7)	17 (11)	−9 (23)	−93 (22)	−58 (23)	−16 (7)							
H(102)	0·80 (3)	0 (8)	−20 (7)	−28 (7)	0 (11)	51 (23)	−113 (22)	39 (22)	−27 (7)							
H(111)	1·03 (3)	−11 (10)	40 (8)	42 (9)	−17 (15)	−41 (28)	−16 (25)	94 (27)	4 (8)							
H(112)	0·96 (3)	31 (8)	49 (8)	−18 (11)	18 (12)	74 (28)	−145 (32)	−18 (27)	−4 (8)							
H(113)	0·99 (3)	−47 (10)	1 (9)	−78 (8)	−1 (15)	12 (28)	65 (28)	−3 (27)	−8 (8)							

As in the case of the neutron intensity data, extinction was not found to be serious. The large neutron crystal gave essentially the same value $g = 0{\cdot}046\,(3) \times 10^4$ rad^{-1} for the isotropic extinction parameter as was presently obtained for the small X-ray crystal, $g = 0{\cdot}039\,(7) \times 10^4$ rad^{-1}. The X-ray reflection most affected was 200, for which the extinction correction was $0{\cdot}94F_c$.

There were systematic discrepancies between corresponding values of anisotropic thermal parameters obtained from the X-ray and neutron data. Agreement was good for all U_{22} values, but in directions normal to the b axis, the mean-square vibrational amplitudes of C and N atoms appear to be systematically smaller by about 10% when determined from the X-ray data. This does not necessarily imply a real difference in the temperatures at which X-ray and neutron data were collected. For parabanic acid (Craven & McMullan, 1979), there were systematic differences with similar relative magnitudes and sense, affecting all U_{ii} values, although in this case, both the X-ray and neutron intensity data were collected at room temperature. Craven & McMullan (1979) have pointed out that others have observed similar effects, with varying magnitudes and sense, and that these have not yet been satisfactorily explained.

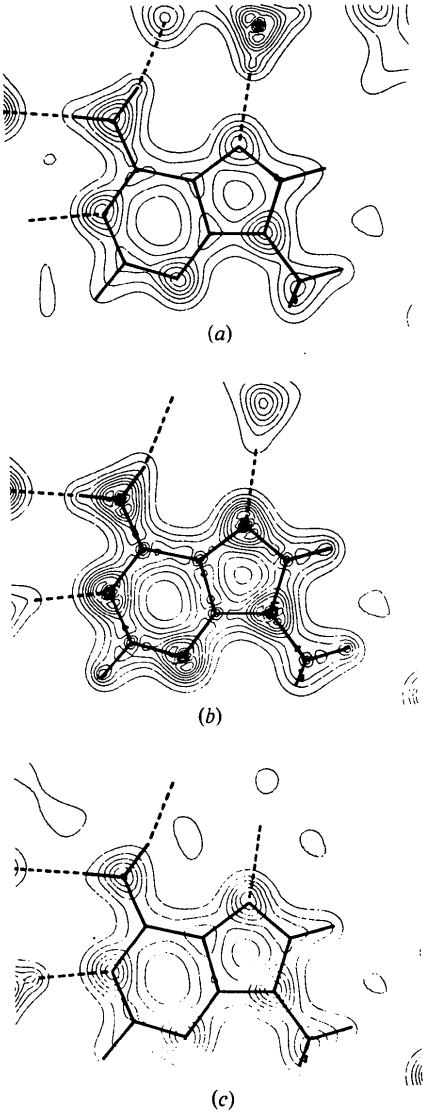

Fig. 2. Total valence charge density for the molecule at rest in the planes as defined in Fig. 1. Contours are at intervals 0·5 e Å^{-3}. The maxima around the N atoms and at the H atoms have an e.s.d. of 0·15 e Å^{-3}.

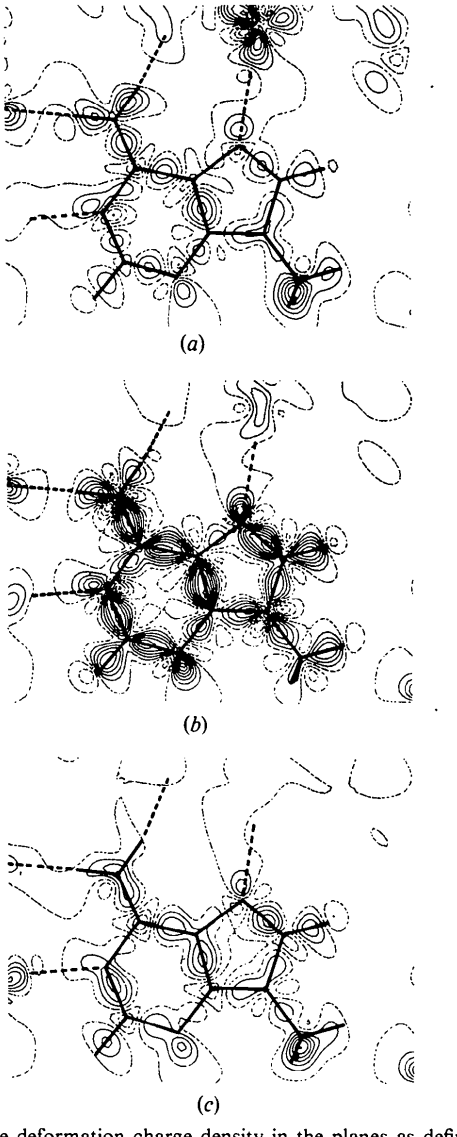

Fig. 3. The deformation charge density in the planes as defined in Fig. 1. Contours are at intervals 0·10 e Å^{-3} with zero and negative contours (charge deficiency) shown as dashed lines. The e.s.d. at the maxima in the deformation density is about 0·05 e Å^{-3}.

In the charge density refinement of 9-methyladenine, the monopole population parameters (p_v) were refined without constraint. The final value, $\sum p_v = 54{\cdot}1\,(2)$ e, for the total valence charge should be 56 e for a neutral molecule. Although the discrepancy seems significant, the result is believed to be satisfactory considering the simple nature of the radial charge density functions which were assumed. The population parameters listed in Table 2 and the valence charge density maps (Figs. 2, 3) have been scaled to provide values for a neutral molecule.

The valence charge density maps (Figs. 2, 3) are the sums of multipole terms for a structure composed of stationary pseudoatoms described by the neutron positional parameters and the population and radial parameters from Table 2. It is thus assumed that the charge density has been properly deconvoluted from the effects of thermal motion. Although it is unlikely that this has been achieved, Stewart (1968) has shown that systematic errors in atomic thermal parameters have their greatest effect at each atom center. At distances beyond 0·3 Å, these effects are considered to be minimal.

Discussion

For 9-methyladenine, the observed distribution of atomic charges is generally consistent with chemical notions of electronegativity (Pauling, 1960). Thus the monopole population parameters (p_v) which represent the net valence charge associated with each pseudoatom indicate that the N atoms are negative, the C atoms neutral or slightly positive, and the H atoms neutral, except for the hydrogen-bonded hydrogens, which are positive. However, caution is needed in interpreting the apparent charge migration between pseudoatoms of different kinds, since this is dependent on the model and particularly on the form of the assumed radial functions. More reliable comparisons can be made regarding the observed charges for pseudoatoms of the same kind. For the nitrogen atoms N(1), N(7) and N(3), with p_v values 5·28, 5·16, 5·08 e (e.s.d. 0·03 e), respectively, the sequence of decreasing charge is consistent with N(1) and N(7) being the preferred sites for hydrogen bonding and protonation of adenine derivatives (Sundaralingam & Jensen, 1965; Voet & Rich, 1970; Bryan & Tomita, 1962) even in crystal structures such as adenine hydrochloride hemihydrate (Cochran, 1951; Kistenmacher & Shigematsu, 1974), where the approach to the N(3) site is unprotected by N(9) substituents.

The deformation density maps (Fig. 3) emphasize directional character in the distribution of bonding and nonbonding electrons, since they contain only the aspherical component of the valence charge about each static nucleus. Thus there is enhancement of charge density in the bonding regions between atoms and in the nonbonding so-called lone-pair regions at nitrogen atoms N(1), N(3) and N(7).* The maximum deformation density 0·73 (5) e Å^{-3} occurs in the C(4)–C(5) bond and in the N(3) nonbonding region. There are ten N–C bonds in the ring system, not counting the bond to the methyl C atom. It might be expected that the deformation density would be greater in the C–N bonds which are stronger, as indicated by the shortening of the C–N bond length. The peak value of the deformation density in each bond can be correlated with the C–N bond length in this way (Fig. 4). Berkovitch-Yellin & Leiserowitz (1977) have noted a similar correlation involving C–C bonds taken from a number of crystal structures. In their study, the deformation charge was integrated over the positive density region. Such a procedure is less satisfactory for more polar bonds such as C–N or C–O where the deformation density may consist of both positive and negative regions and the boundary of the bonding region is poorly defined.

Perhaps the most interesting and important aspect of the valence charge density in 9-methyladenine involves the H atoms. There are two hydrogen bonds NH(101)···N(1)′ and NH(102)···N(7)″ which are weak, like other hydrogen bonds formed in crystal structures when adenine derivatives are self-associated (Hsu & Craven, 1974). The distances are 2·96 and

* Density differences in the sections above and below the molecule [Figs. 2(*a*) *vs.* 2(*c*), and Figs. 3(*a*) *vs.* 3(*c*)] are attributed to the nonplanarity of the molecule. The C and N nuclei are displaced in the range ±0·025 Å from the best least-squares plane. The H nuclei are displaced H(2) −0·051, H(8) −0·046, H(101) 0·243, H(102), 0·099, H(111) 0·108, H(112) −0·931, H(113) 0·833 (2) Å from this plane, according to MBC. Thus the H(102) nucleus is almost midway between sections Fig. 2(*a,b*) and Fig. 3(*a,b*).

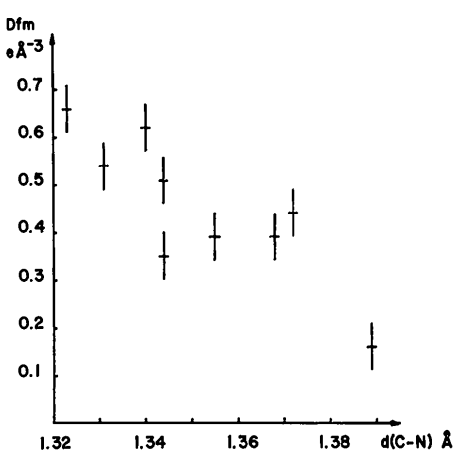

Fig. 4. The maximum deformation density (e Å^{-3}) in each C–N bond plotted *versus* the bond length. The N(9)–C(11) bond is excluded. Lines through the points are of length ±σ.

3·06 Å* for N···N(1)′ and N···N(7)″, 1·95 and 2·04 Å for H(101)···N(1)′ with angles 166 and 176° at the H atoms. There is also a close interaction C(11)–H(111)···N(3)′ involving two molecules in the same sheet (Fig. 2, MBC). The distances are 3·35 Å for C···N, 2·52 Å for H···N with angle 133° at the methyl H atom. Although the H···N distance is shorter than the van der Waals distance (2·7 Å; Pauling, 1960), this interaction is not regarded as a hydrogen bond.

There are systematic differences in the charge density at the C–H and N–H hydrogen atoms which affect the net charge and the dipole deformation of the charge about each proton. The C–H hydrogen atoms of the ring system and the methyl group have p_v values within a narrow range 0·96 to 1·05 e, with an average value 1·01 e. None of the net charges on these atoms is significant, including the value +0·03 (3) e for the atom H(111) which is involved in the short C–H···N interaction. However, the N–H hydrogen atoms are both significantly positive, with charges +0·23 and +0·20 (3) e. As pointed out above, care is necessary in attributing physical significance to the partitioning of charge between different atoms, as in the N–H···N and C–H···N groups. Nevertheless, it is noted that in both the N–H···N hydrogen bonds the charges on the proton donor, −0·23 (3) e, and acceptor nitrogens, −0·28, −0·16 (3) e, are all negative and the bridging hydrogen is positive, whereas in the C–H···N interaction, the charges on the C and N atoms are marginally positive, +0·17 (4) e, and negative, −0·08 (3) e, respectively, and the bridging H atom is neutral. The resulting Coulombic interactions within these groupings are attractive in each case, but are weaker for C–H···N. The charge distribution in the N–H···N groups is consistent with longstanding theory (Coulson & Danielsson, 1955) concerning the importance of the electrostatic contribution to hydrogen bonding. More recent *ab initio* molecular-orbital calculations (Kollman & Allen, 1971) for an isolated ammonia molecule, give net atomic charges which are greater than those observed in 9-methyladenine, with +0·30 e at the H atoms and −0·90 e at the N. When a hydrogen-bonded ammonia dimer is formed so as to maintain the rigid monomer geometry, the greatest change in an atomic charge is +0·03 e, and this occurs at the bridging hydrogen. The magnitude of the charge shift is comparable to the e.s.d. in the p_v values obtained for 9-methyladenine. This would suggest that the hydrogen bonding in the crystal structure has little or perhaps no apparent effect on the observed distribution of net charges in the molecule.

* Distances are quoted with two significant figures, although the apparent e.s.d.'s are small (0·001 Å). This is because intermolecular distances are subject to thermal-elongation corrections which are uncertain, but could be 0·005 Å in this case.

Table 3. *Dipole deformations at* H *atoms*

The magnitude $|d|$ is given by $(d_1^2 + d_2^2 + d_3^2)^{1/2}$ where d_j are the population parameters from Table 2. The value $d_{H\rightarrow X}$ is the component of d along the covalent bond vector H–C or H–N. All are positive values, indicating enhancement of electronic charge in the bonding region. The angle φ is between the bond vector H–C and H–N and the direction of the maximum deformation at each H center.

Atom Bond	$\lvert d\rvert \times 10^2$	$d_{H\rightarrow X} \times 10^2$	φ (°)
H(2)–C(2)	76 (11)	72 (8)	19 (6)
H(8)–C(8)	80 (11)	78 (8)	12 (6)
H(101)–N(10)	32 (11)	28 (8)	29 (14)
H(102)–N(10)	35 (11)	32 (8)	23 (13)
H(111)–C(11)	59 (16)	53 (9)	26 (9)
H(112)–C(11)	60 (16)	49 (9)	35 (9)
H(113)–C(11)	91 (16)	89 (9)	11 (6)

An unexpected feature of the charge distribution at the H atoms was found (Table 3) when comparing the population parameters for the dipole deformations (d_j in Table 2). At every H atom, there is a polarization in the sense which enhances the charge in the C–H or N–H bond. The effect is to deshield the proton on the side which is exposed to the molecular environment. This would favor stronger interaction with nearby electronegative atoms, as in N–H···N hydrogen bonding. It is surprising that the effect is only marginally significant for the N–H hydrogen atoms, but is highly significant for the C–H hydrogen atoms, particularly for H(2) and H(8), which are bonded to ring atoms. For the atom H(111), which is involved in the C–H···N interaction, the dipole deformation is of intermediate strength. The relative magnitudes of these dipole deformations can also be seen in the maps (Fig. 3). Such effects do not appear to have been noted in previous combined X-ray and neutron studies of molecules containing both C–H and N–H groups. In 9-methyladenine, both hydrogen bonds are long. In other crystal structures with stronger hydrogen bonds, the dipole deformation at the bridging proton may become more important. There are several examples of close C–H···O interactions involving the C(8) position in purines. Rosenberg, Seeman, Kim, Suddath, Nicholas & Rich (1973) report C(8)···O(5′) intramolecular distances such as 3·07 Å in adenylic acid derivatives and, in a crystal complex, there is a distance 3·16 Å between atom C(8) of caffeine and a carbonyl O atom of barbital (Craven & Gartland, 1970). In 9-methyladenine, there is no unusual interaction at C(8). However, the dipole deformation at H(8) may be characteristic of purines, and may be a contributing factor in the formation of the short C–H···O distances.

We thank Dr J. R. Ruble for assistance with the X-ray data collection, and Dr R. F. Stewart for his sustaining interest. The work was supported by Grants

GM-22548 from the National Institutes of Health, and CHE-77-09649 from the National Science Foundation.

References

BECKER, P. J. & COPPENS, P. (1974). *Acta Cryst.* A**30**, 129–147.

BERKOVITCH-YELLIN, Z. & LEISEROWITZ, L. (1977). *J. Am. Chem. Soc.* **99**, 6106–6107.

BRYAN, R. F. & TOMITA, K. (1962). *Acta Cryst.* **15**, 1179–1182.

BUSING, W. R. & LEVY, H. A. (1957). *Acta Cryst.* **10**, 180–182.

CLEMENTI, E. (1965). *IBM J. Res. Dev. Suppl.* **9**, 2.

COCHRAN, W. (1951). *Acta Cryst.* **4**, 81–92.

COULSON, C. A. & DANIELSSON, U. (1955). *Ark. Fys.* **8**, 239–255.

CRAVEN, B. M. & GARTLAND, G. L. (1970). *J. Pharm. Sci.* **59**, 1666–1670.

CRAVEN, B. M. & MCMULLAN, R. K. (1979). *Acta Cryst.* B**35**, 934–945.

CRAVEN, B. M. & WEBER, H. P. (1977). *The POP Least-Squares Refinement Procedure*, Tech. Rep. Crystallography Department, Univ. of Pittsburgh.

HAMILTON, W. C. (1974). *International Tables for X-ray Crystallography*, Vol. IV, pp. 285–310. Birmingham: Kynoch Press.

HSU, I-N. & CRAVEN, B. M. (1974). *Acta Cryst.* B**30**, 988–993.

KISTENMACHER, T. J. & ROSSI, M. (1977). *Acta Cryst.* B**33**, 253–256.

KISTENMACHER, T. J. & SHIGEMATSU, T. (1974). *Acta Cryst.* B**30**, 166–168.

KOLLMAN, P. A. & ALLEN, L. C. (1971). *J. Am. Chem. Soc.* **93**, 4991–5000.

MCMULLAN, R. K., BENCI, P. & CRAVEN, B. M. (1980). *Acta Cryst.* B**36**, 1424–1430.

PAULING, L. (1960). *The Nature of the Chemical Bond*, 3rd ed. Ithaca: Cornell Univ. Press.

ROSENBERG, J. M., SEEMAN, N. C., KIM, J. J. P., SUDDATH, F. L., NICHOLAS, H. G. & RICH, A. (1973). *Nature (London)*, **243**, 150–154.

STEWART, R. F. (1968). *Acta Cryst.* A**24**, 497–505.

STEWART, R. F. (1976). *Acta Cryst.* A**32**, 565–574.

STEWART, R. F. & JENSEN, L. H. (1964). *J. Chem. Phys.* **40**, 2071–2075.

SUNDARALINGAM, M. & JENSEN, L. H. (1965). *J. Mol. Biol.* **13**, 930–943.

VOET, D. & RICH, A. (1970). *Prog. Nucleic Acid Res. Mol. Biol.* **10**, 183–265.

Acta Cryst. (1981). B**37**, 1591–1596

Structure of *N*-Acetyl-L-cysteine: X-ray ($T = 295$ K)* and Neutron ($T = 16$ K)† Diffraction Studies

BY FUSAO TAKUSAGAWA AND THOMAS F. KOETZLE‡

Chemistry Department, Brookhaven National Laboratory, Upton, New York 11973, *USA*

W. W. H. KOU AND R. PARTHASARATHY‡

Center for Crystallographic Research, Roswell Park Memorial Institute, Buffalo, New York 14203, *USA*

(*Received* 27 *October* 1980; *accepted* 10 *February* 1981)

Abstract

N-Acetyl-L-cysteine, $C_5H_9NO_3S$, $M_r = 163{\cdot}20$, crystallizes in the space group $P1$, with $a = 5{\cdot}766$ (1), $b = 6{\cdot}433$ (1), $c = 5{\cdot}014$ (1) Å, $\alpha = 102{\cdot}80$ (2), $\beta = 102{\cdot}77$ (1), $\gamma = 95{\cdot}81$ (1)°, $Z = 1$ and final $R(F^2) = 0{\cdot}024$ for a total of 1232 independent reflections, at $T = 16$ K. The structure was first deduced from X-ray data obtained at 295 K. A subsequent neutron diffraction study carried out at 16 K has provided a more precise description of the hydrogen bonds than was possible from the X-ray experiment. The thiol group acts as both donor and acceptor, being involved in S–H···O and N–H···S interactions.

Introduction

The thiol or sulfhydryl group in cysteine residues has attracted a great deal of attention because of its ability to take part in a variety of biochemical reactions (Friedman, 1973; Jocelyn, 1972). The role of the thiol group as a possible hydrogen-bond donor and acceptor has been explored in a number of studies (Gordy &

* Structure and Conformation of Amino Acids Containing Sulfur. IV. Work supported by NCI, CA 23704.

† Precision Neutron Diffraction Structure Determination of Protein and Nucleic Acid Components. XIX. Part XVIII: Kvick, Canning, Koetzle & Williams (1980). Research carried out under contract with the US Department of Energy, and supported by its Office of Basic Energy Sciences.

‡ To whom correspondence should be addressed.

0567-7408/81/081591-06$01.00